FOI-R–0367–SE
Jan 2002
ISSN 1650-1942

Technical report

Jeroen Wackers

Position of a Small Fin on a Missile Body for Maximum Directional Stability

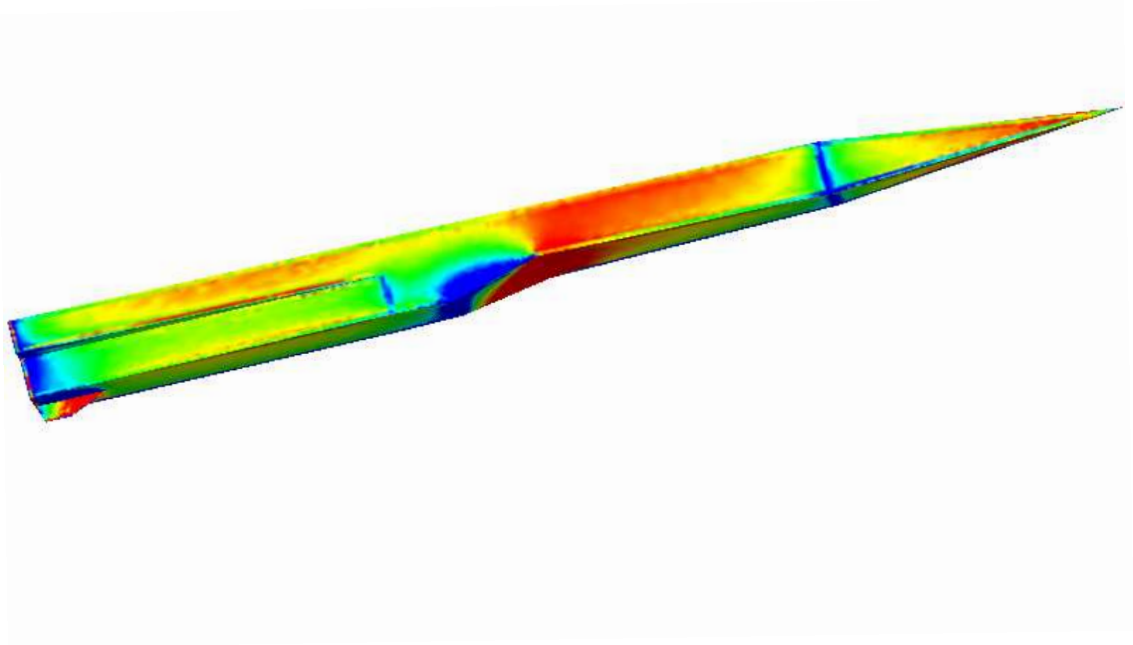

Division of Aeronautics, FFA
SE-172 90 STOCKHOLM

FOI – Swedish Defence Research Agency
Division of Aeronautics, FFA
SE-172 90 STOCKHOLM

FOI-R–0367–SE
Jan 2002
ISSN 1650-1942

Technical report

Jeroen Wackers

Position of a Small Fin on a Missile Body for Maximum Directional Stability

Division of Aeronautics, FFA
SE-172 90 STOCKHOLM

Abstract

Windtunnel measurements and CFD calculations were performed to determine the position of a small fin on a missile body that gives the highest directional stability. The model used is the configuration KROPP of the Tvärteknikprojekt, a concept for a future heavy cruise missile.

For supersonic speeds, the fin creates a shock pattern behind itself on the body. The generated pressure differences contribute to the yawing moment at sideslip, so much that it is advantageous to move the fin forward on the body. Although this decreases the effect of the fin itself (because of a shorter moment arm), it increases the total moment. The maximum yawing moment is encountered when the entire shock pattern is placed on the body. A 35% increase in yawing moment due to fin was noted.

For subsonic speeds this effect is smaller, because the fin influences a smaller part of the body. The yawing moment does not vary much with fin position. The best position is most probably with the trailing edge a short distance away from the base.

Contents

List of symbols

α	angle of attack (wind from below = positive)
β	angle of sideslip (wind from starbord = positive)
μ	Mach angle = $\arcsin\left(\frac{1}{M}\right)$
ρ	freestream density
C_C	side force coefficient = $\frac{\text{side force}}{qS_{ref}}$ (to port = positive)
C_{C_β}	$\frac{\partial C_C}{\partial \beta}$
C_n	yawing moment coefficient = $\frac{\text{yawing moment}}{qS_{ref}l_{ref}}$ (nose to starbord = positive)
C_{n_β}	$\frac{\partial C_n}{\partial \beta}$
C_p	pressure coefficient = $\frac{p-p_\infty}{q}$
l_{ref}	reference length, diameter of warhead = 0.35 m
M	freestream Mach number
p	static pressure
p_∞	freestream static pressure
q	freestream dynamic pressure = $\frac{1}{2}\rho V^2$
S_{ref}	reference area, cross-section of warhead = $\frac{\pi l_{ref}^2}{4}$ = 0.0962 m^2
V	freestream velocity
X	coordinate from a point above the nose straight back
X_{ref}	X-coordinate of reference point = 4.00 m

1 Introduction

A fin that is attached to an aircraft or missile body interacts aerodynamically with this body, making the fin more effective. The pressure difference caused by the fin at sideslip is transferred to the body, resulting in a pressure difference on the body as well. In its turn, the body acts as an endplate to the fin, increasing its lift. These effects together produce a larger sideforce and yawing moment due to sideslip than the fin alone would have produced.

A fin is usually placed at the end of the body, to maximize its moment arm. But when a small fin is placed on a large body, the moment produced by the body may be so large that when the fin is moved *forward*, the total moment increases. The fin moment arm is reduced, but the fin influences a larger body area so the body moment increases. When the sum of these effects is positive, the total moment increases.

Windtunnel tests were performed for the Tvärteknikprojekt at FOI, Aeronautics Division FFA, on a model of a future heavy cruise missile. The model was equipped with a small fin under the body to increase directional stability. During the tests, the effect mentioned above was noted. It was then decided to investigate the effect of the fin's position further using CFD. This report describes CFD and windtunnel results for both subsonic and supersonic speeds. The optimum position of the fin is derived from these.

The report starts with a description of the CFD model and windtunnel model used and their differences (chapter 2). The next chapter describes the CFD calculations and the grids that were used. Chapter 4 gives results for supersonic speeds. The flow pattern is analyzed, CFD and windtunnel forces are compared and the optimum position of the fin is determined. Chapter 5 does the same, but now for subsonic speeds. The report ends with a conclusion.

2 Missile geometry

Both windtunnel tests and CFD calculations were performed on the windtunnel model geometry for the Tvärteknikprojekt, configuration KROPP, with small fin, as described by Johansson et al. [4]. On the windtunnel model, the fin was placed in two different positions, CFD calculations were performed for four different positions.

The geometry for the windtunnel model differs somewhat from the CFD geometry. Both are presented here.

2.1 CFD Model

The CFD model has a length of 7500 mm, a straight base and sharp edges. It is shown in figure 1. Calculations were performed with the small fin in four different positions, with its trailing edge at 0, 25, 50 and 75 cm from the base. These four configurations are shown in figure 2.

Figure 1. KROPP CFD geometry, from [4].

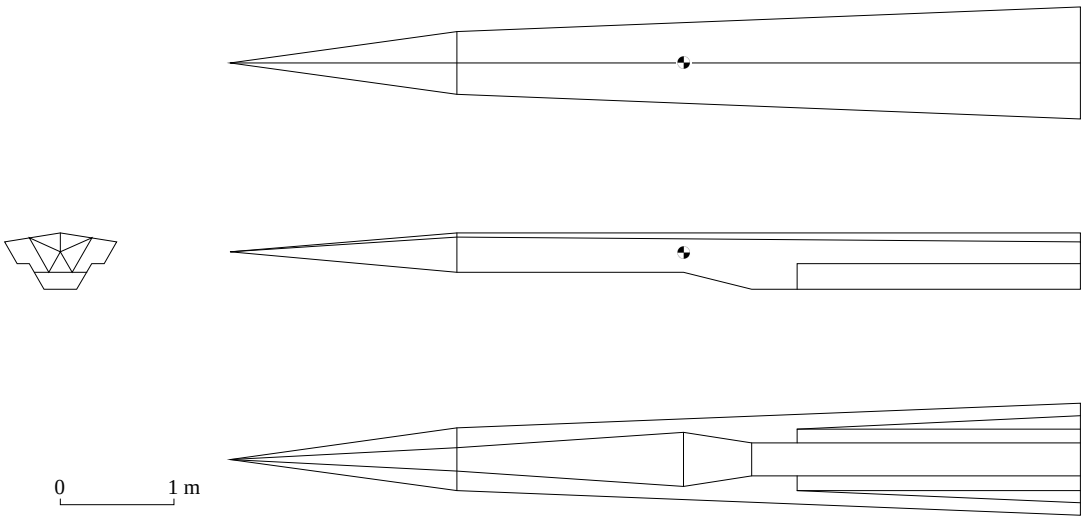

Figure 2. KROPP with 4 different fins, CFD geometry. Configurations are named after the distance between the base and the fin trailing edge.

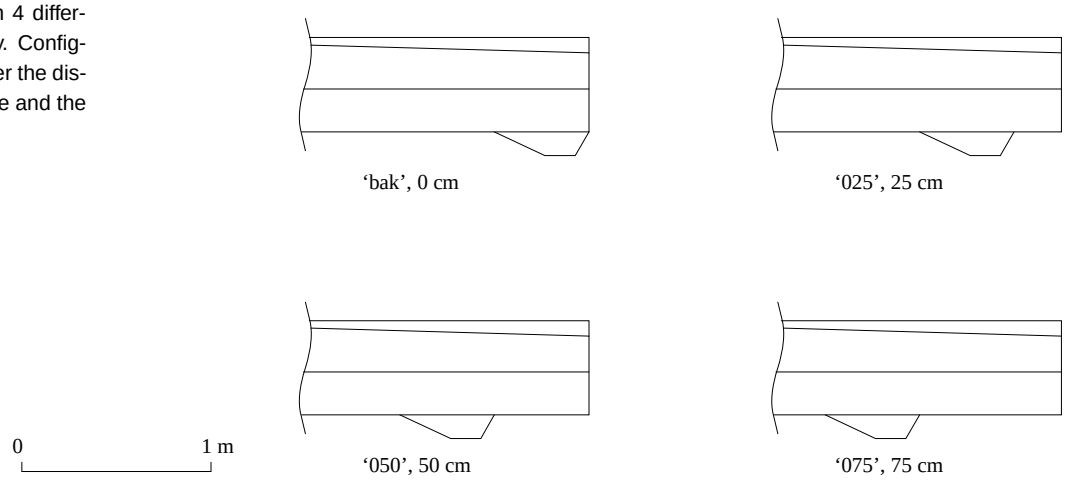

2.2 Windtunnel model

The windtunnel model is not the same as the CFD model. The 1:18 model would have a full-scale length of 7668 mm, it has a tapered base, the edges on the underside are rounded (figure 3) and the aftmost part of the upper side is flat. However, the reference point is the same.

The fin has been tested in two different positions: the ‘standard’ position at 48.6 cm from the base end (full scale) and the ‘bak’ position with the trailing edge at the base (figure 4). Note that these configurations have 168 mm longer moment arms than the corresponding CFD configurations ‘bak’ and ‘050’, because the body is longer.

Figure 3. KROPP windtunnel geometry.

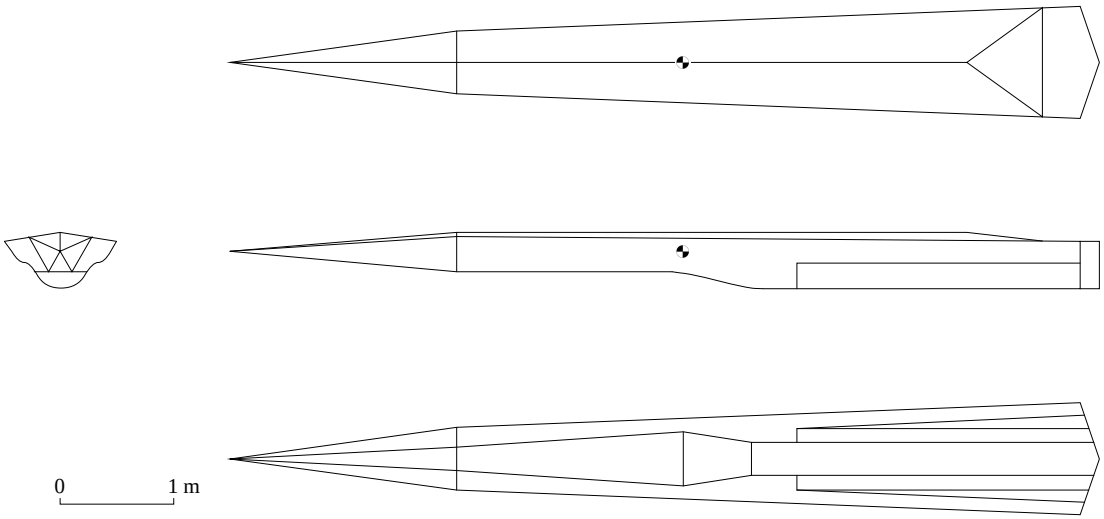

Figure 4. KROPP with 4 different fins, Windtunnel model geometry. Most windtunnel tests were run with the ‘standard’ configuration.

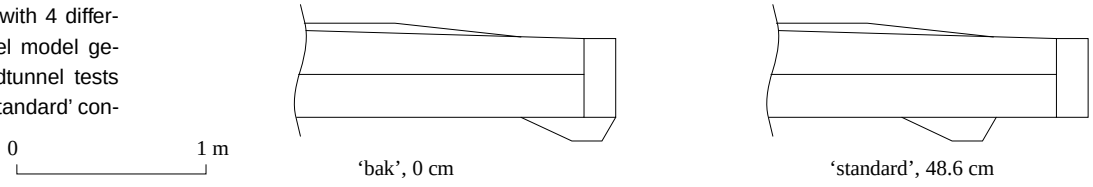

3 CFD calculations

Software Calculations were performed on an unstructured grid using FFA's unstructured solver EDGE [1]. All geometries were created with the structured grid program FFANET [2] and unstructured grids were created with Tritet [3]. All CFD calculations are solutions of the Euler equations, that means viscosity effects are neglected.

Grids The basic grids have about 38,000 nodes each. These showed sufficient accuracy for M 1.5: asymmetric forces and moments are very close to zero for $\beta = 0$ and a calculation with a 100,000 node grid for one of the cases gave very small differences with the 38,000 node calculation.

Accuracy for M 0.5, however, was insufficient. This is most probably caused by the base flow, which is not smooth and thus requires many cells for an accurate solution. For $M = 1.5$, the base flow can not influence the flow around the missile itself.

To improve accuracy, all $M = 0.5$ cases were calculated with flow-adapted grids. After the flow was calculated on the basic grid, a new grid was created for every flow case with small cells in places with strong gradients. These grids had a typical size of 75,000 nodes. They showed sufficiently small asymmetric forces for $\beta = 0$.

4 Effects of fi n position, Mach 1.5

When the missile is flying at a supersonic speed, the fin basically influences only that part of the body that lies behind it. Therefore, moving the fin forward can be very effective. This chapter shows the flow pattern caused by the fin first, then the resulting moments are discussed for both CFD and windtunnel results.

4.1 Flow pattern

Pressure 'lanes' When the missile has a certain sideslip, the fin looks like a wing under an angle of attack. The leading edge produces two waves: a shock on the windward side and an expansion on the leeward side, causing a higher pressure on the windward side and a lower pressure on the leeward side. The trailing edge produces an expansion on the windward side and a shock on the leeward side, such that the pressures behind the fin are equal. Thus, the fin causes two 'lanes' of high and low pressure that run into the flow.

The more forward the fin is placed, the larger the body area that is covered by these lanes (up to a limit). Pressure plots from CFD calculations show the forward movement of the high- and low-pressure areas when the fin is moved forward (figures 5 to 8). For the fin at 25 cm, only the lower part of the body is covered, for 50 cm the upper part is covered as well. If the fin is placed at more than 50 cm the total covered area does not change anymore, it just moves forward.

Note that the pressure in the influenced regions does not change much when the fin is moved and that the induced pressure in the lanes does not really decrease for areas farther away from the fin (the colours in the lanes are almost the same).

When the flow pictures are compared with a picture showing C_p for the body without any fin (figure 9), it is obvious that the fin really influences the lanes only. The pressure in front of the fin does not change, because the flow is supersonic, but even the pressure behind the lanes shows no big changes. Only a slightly lower pressure is formed directly behind the fin (visible in figures 7 and 8).

Mach line estimate To estimate the pressure lane location, the Mach angle μ can be used. The simplest possible approximation of the waves are the Mach lines at $\beta = 0$, that means the lines with direction $\mathbf{x}$ that satisfy:

$$\mathbf{x} \cdot \begin{pmatrix} 1 \\ 0 \\ 0 \end{pmatrix} = \cos(\mu)$$

Finding this lines on the body surface gives the wave locations.

This method does not take into account the finite strength of the waves, nor the change in freestream direction for non-zero β (although this can be done by taking the inner product of $\mathbf{x}$ with the freestream velocity). Figures 5 to 8 show however that even the simplest approximation gives good results.

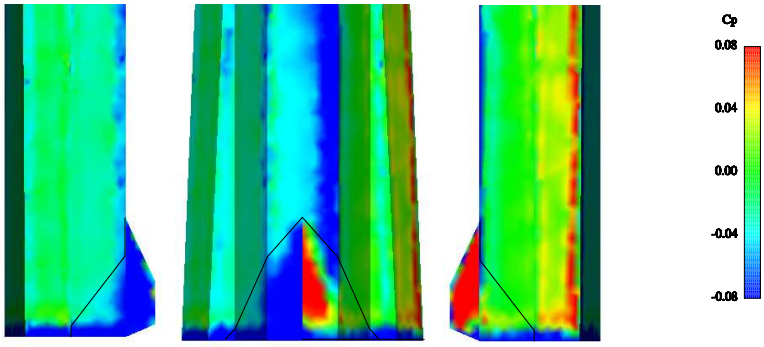

Figure 5. KROPP afterbody, fin at the base. C_p. Black lines indicate Mach lines on the surface for M = 1.5, μ = 41.8 deg. α = 0 deg, β = -10 deg.

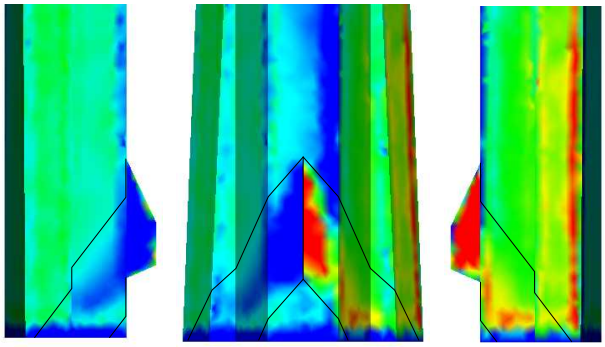

Figure 6. KROPP afterbody, fin at 25 cm. C_p. Black lines indicate Mach lines on the surface for M = 1.5, μ = 41.8 deg. α = 0 deg, β = -10 deg.

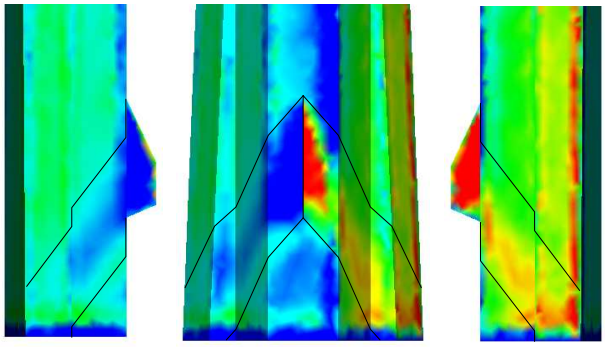

Figure 7. KROPP afterbody, fin at 50 cm. C_p. Black lines indicate Mach lines on the surface for M = 1.5, μ = 41.8 deg. α = 0 deg, β = -10 deg.

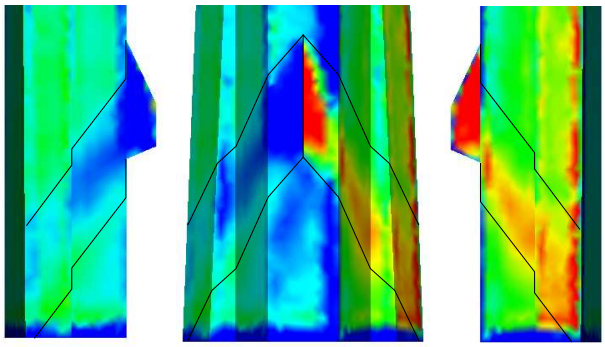

Figure 8. KROPP afterbody, fin at 75 cm. C_p. Black lines indicate Mach lines on the surface for M = 1.5, μ = 41.8 deg. α = 0 deg, β = -10 deg.

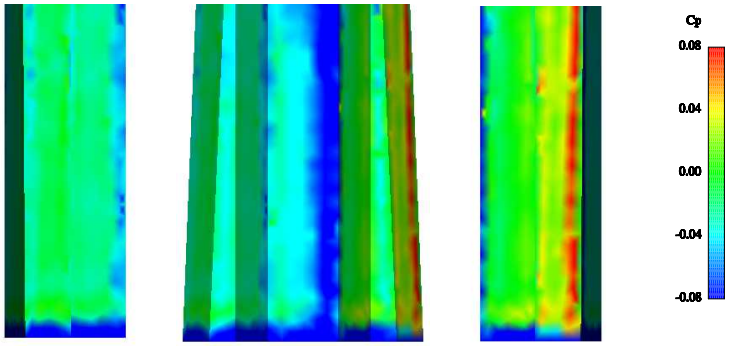

Figure 9. KROPP afterbody, no fin. M = 1.5. α = 0 deg, β = -10 deg.

4.2 Side force and yawing moment

The effect of the small fin on sideforce and yawing moment coefficients from CFD follows from figures 10 and 11. Adding a fin to the body causes a small increase in side force and a rather large increase in yawing moment, from unstable to almost stable.

Dependence on fin position The effect of the fin's position follows from these figures and also from figures 14 and 15, which show the incremental effect of the fin. Side force increases with fin distance from the base: the larger the body area that is influenced by the fin, the larger the side force created by the body. The side force caused by the fin itself does not change, because the flow is supersonic, so changes in geometry behind the fin do not affect the fin (changes in the flow field in front of the fin have an influence, but the flow field on the last part of the body is almost uniform so this influence is small). Once the fin waves are free from the base, the total side force will not change much anymore (this happens for 75 cm or more, see figure 8).

The yawing moment, however, reaches a maximum. When the fin is moved forward, the influenced body area increases but the fin moment arm decreases (at 50 cm from the base, the moment arm (reference point to the fin's mid root chord) is decreased from 3.19 m to 2.69 m, a reduction of 16%). The figures show that the yawing moment continues to grow with fin distance from the base until the influenced body area becomes constant, which happens between 50 and 75 cm. It is interesting to see that for 5 deg β the 50 cm fin is better, but for 10 deg β the 75 cm fin gives a higher C_n. For this angle, the flow pattern is rotated more than for 5 deg, so the high-pressure 'lane' is moved backward and the total influenced area is still increasing at 75 cm (figure 8).

Force and moment derivatives Consider now a side force and yawing moment derivative, approximated by taking the difference in force/moment due to fin at 5 deg and 0 deg or at 10 deg and 5 deg, and dividing this by 5 deg (thus approximating the derivatives of figures 14 and 15). These derivatives are given in figures 16 and 17. They show the same trends as the previous figures: side force increases and levels off, yawing moment increases and then decreases. For 5 - 10 deg this all happens a little later than for 0 - 5 deg.

The first increase looks perfectly linear. It is, however, expected that the curves will become a number of straight lines with different slopes instead of

one line when more cases are calculated. This happens because the increase of influenced body area is not constant. When the shocks advance over a horizontal surface, the vertical influenced area does not change, so C_n increases less or not at all.

Windtunnel results Windtunnel data are compared with CFD in figures 12 and 13. Fin delta effects are given in figures 14 and 15 and derivatives in figures 16 and 17. The windtunnel results differ from the CFD calculations. Most obvious: the effect of a fin is much larger. This is partially caused by viscosity effects and calculation or measurement errors, but also by geometric differences. The windtunnel model has a 5% longer moment arm and a round lower body, so the large pressure differences close to the fin cause a horizontal force.

But measurements and calculations agree qualitatively. The shape of the curves is the same, the fin delta curves (figures 14 and 15) are almost straight (the slopes for 5 - 10 deg are somewhat smaller).

The optimum position of the fin can not be found from the windtunnel results, because only two fin positions were measured. But from the qualitative agreement with CFD it is expected that the flow pattern resembles the calculated pattern and thus that the optimum position lies close to the CFD optimum.

Best fin position In this case, the largest yawing moment is obtained when the shock pattern from the fin does not reach the base, that means the fin trailing edge must be somewhere between 50 and 75 cm from the base. This gives a calculated $\Delta C_{n_{\beta,fin}}$ of 0.21, which is 35% higher than for a fin at the base. Windtunnel results show a maximum $\Delta C_{n_{\beta,fin}}$ of 0.37 (forward position).

Figure 10. Side force coefficient C_C versus β for α = 0, M = 1.5. Five different CFD calculations.

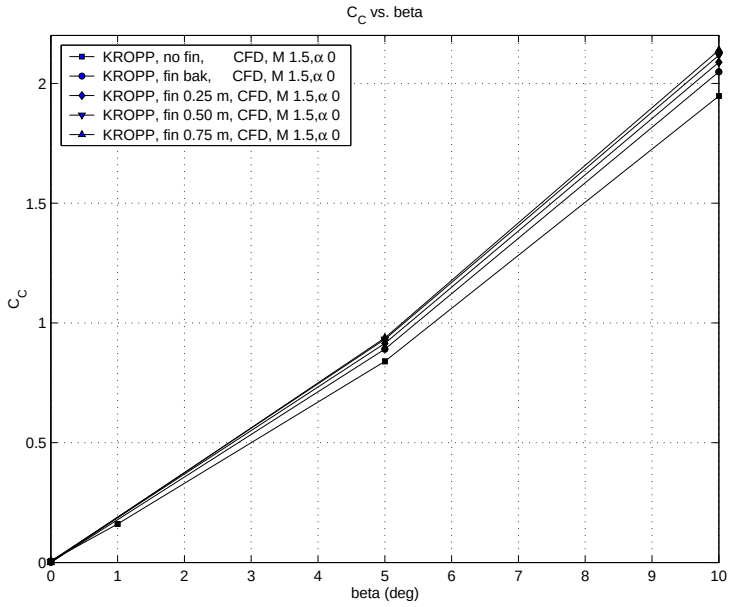

Figure 11. Yawing moment coefficient C_n versus β for α = 0, M = 1.5. Five different CFD calculations.

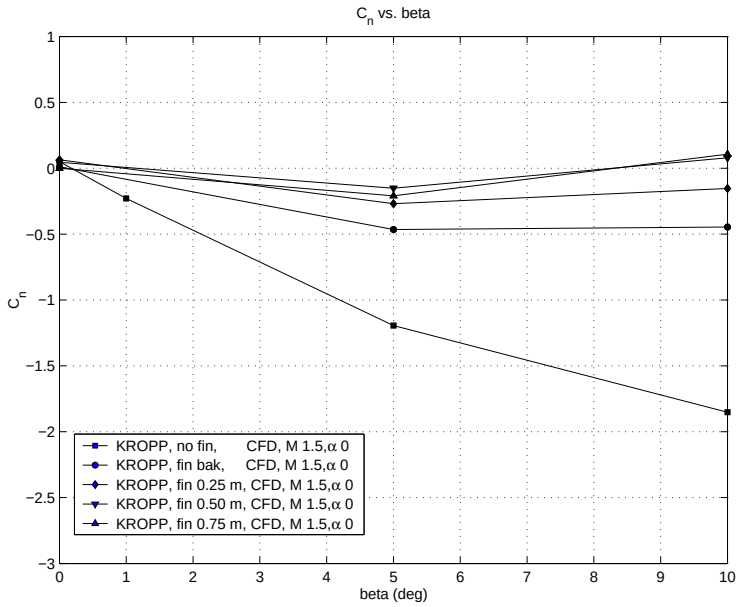

Figure 12. Side force coefficient C_C versus β for α = 0, M = 1.5. Comparison CFD – windtunnel.

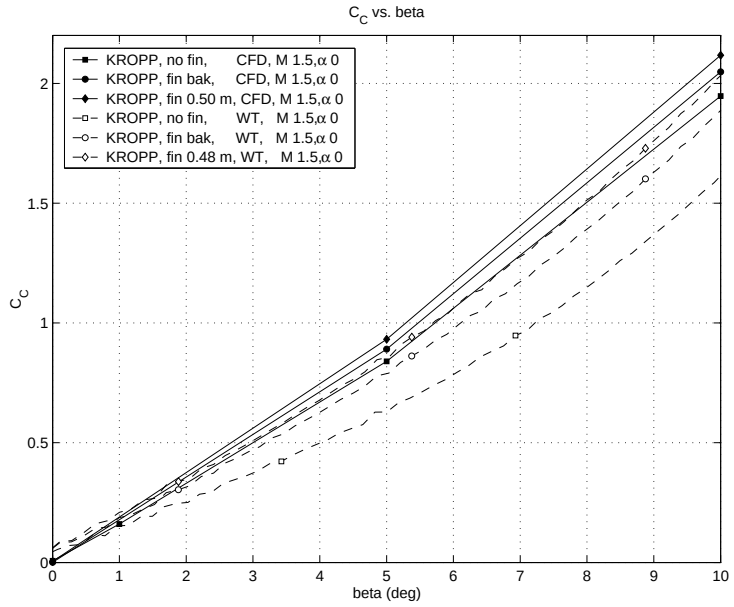

Figure 13. Yawing moment coefficient C_n versus β for α = 0, M = 1.5. Comparison CFD – windtunnel.

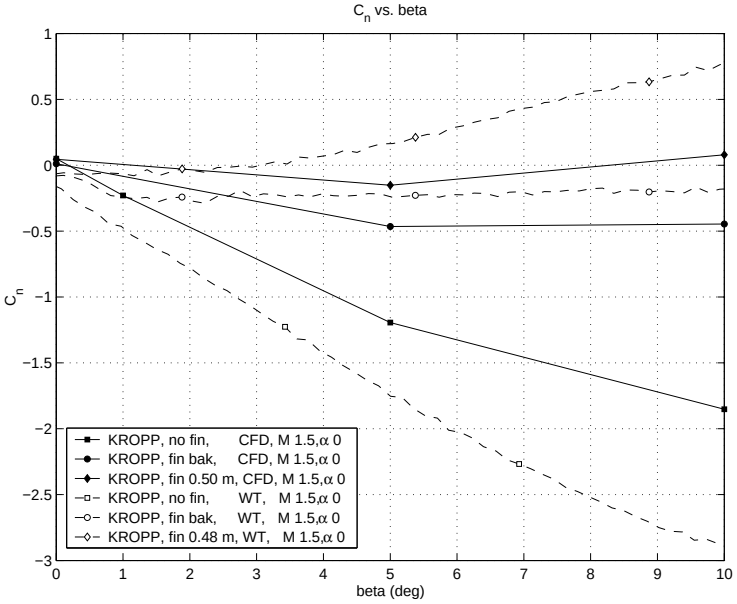

Figure 14. Side force coefficient with fin minus without fin, $\Delta C_{C,fin}$, versus β for α = 0, M = 1.5.

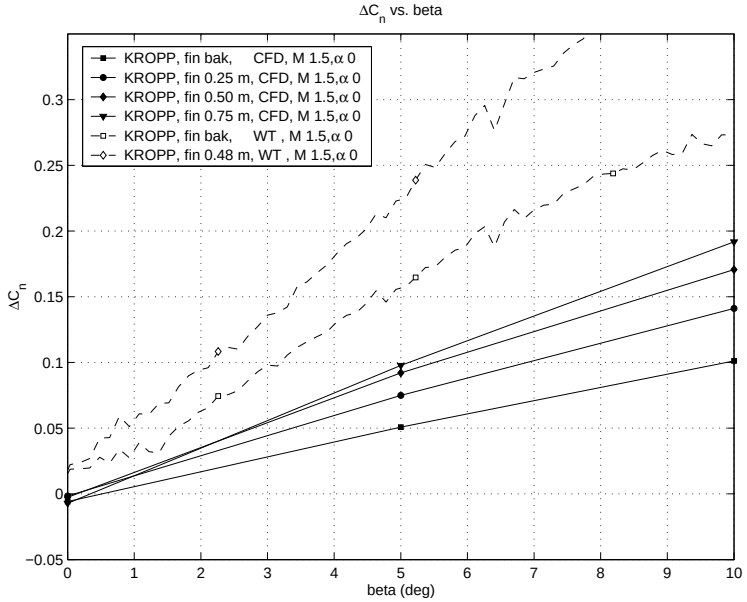

Figure 15. Yawing moment coefficient with fin minus without fin, $\Delta C_{n,fin}$, versus β for α = 0, M = 1.5.

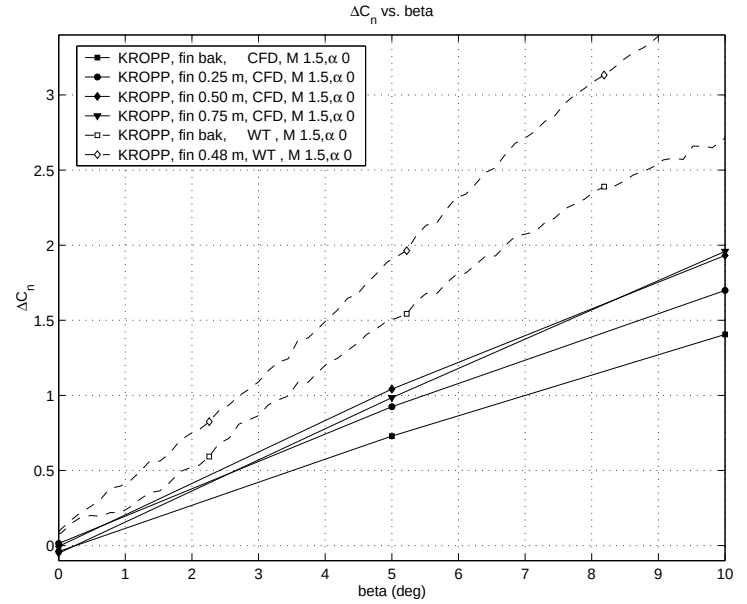

Figure 16. Side force derivative caused by fin, $\Delta C_{C_{\beta,fin}}$, versus distance base – fin trailing edge. α = 0, M = 1.5.

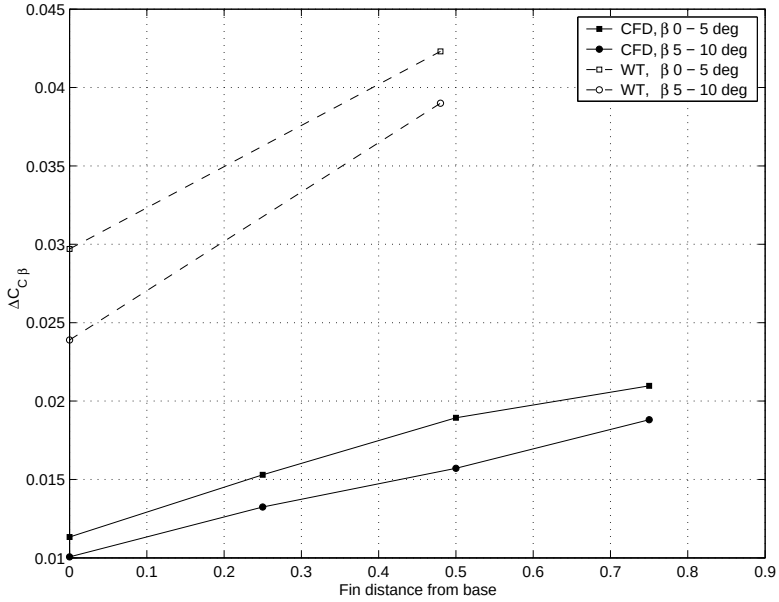

Figure 17. Yawing moment derivative caused by fin, $\Delta C_{n_{\beta,fin}}$, versus distance base – fin trailing edge. α = 0, M = 1.5.

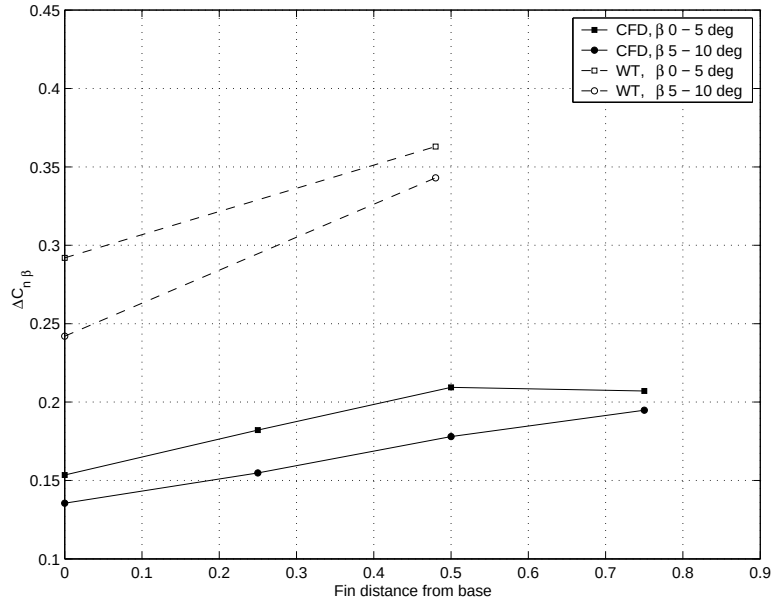

5 Effects of fi n position, Mach 0.5

For speeds lower than the speed of sound, the fin influences the missile body both behind and in front. This influence, however, is less than for supersonic speeds. This chapter shows the flow pattern as well as calculated and measured forces on the missile for M = 0.5.

5.1 Flow pattern

Flow pictures were made using the CFD results for M = 0.5 (figures 18 to 21). To show the fin influence on the body as clearly as possible, a colour scale was used that is different from the scale for M = 1.5. Note that this scale has a maximum C_p of 0, that means freestream pressure. Pressures on the fin and a part of the windward (port) side of the body are ‘off the scale’.

The influence of the fin is not restricted to distinct ’lanes’, but the influenced part of the body lies around the fin. The flow figures show that this influenced area is smaller than for the supersonic case.

A distinct region with high and low pressures exists around the fin on the lower part of the body. This region moves with the fin and does not change much in shape, except when it lies in the low-pressure zone around the base. The pressure near the trailing edge is reduced there for both sides of the fin. (Compare figure 18 with figure 21: figure 18 shows a green area on the port side of the fin that is red in figure 21 and a blue area on the starbord side that is green in figure 21.)

This region does not produce any yawing moment itself, but it influences the pressure distribution on the fin and the body side surfaces.

The fin has a small influence on the lower sides of the body. Figure 18 shows, on the left side of the body, an extension of the yellow – red area compared with the other figures. Figures 19 to 21 show a darker red area next to the fin, as well as a greener area on the right side.

Comparing the flow pictures with one for the body without fin (figure 22), we see that the pressure on the upper sides of the body does not change notably. This means that only the lower sides of the body contribute to the side force and yawing moment. The same picture shows that the influence of the fin is really limited to the body area close to it: the rest of the body pressure does not change.

5.2 Side force and yawing moment

Just like in the supersonic case, the addition of a fin stabilizes the body. Both windtunnel results and CFD calculations show however that the generated yawing moment does not depend much on the position of the fin.

Windtunnel results Windtunnel measurements were again performed for two different positions: with the fin trailing edge at the base and at 48 cm from the base. These positions give almost exactly the same side force and yawing moment (figures 25 and 26). It is thus expected from the windtunnel results that the effect of the fin does not change much with its position. There might be an optimum position between 0 and 48 cm.

Figure 18. KROPP afterbody, fin at the base. C_p. M = 0.5. α = 0 deg, β = -10 deg.

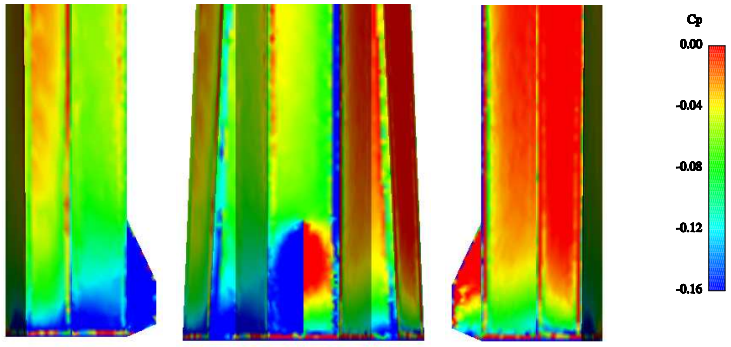

Figure 19. KROPP afterbody, fin at 25 cm. C_p. M = 0.5. α = 0 deg, β = -10 deg.

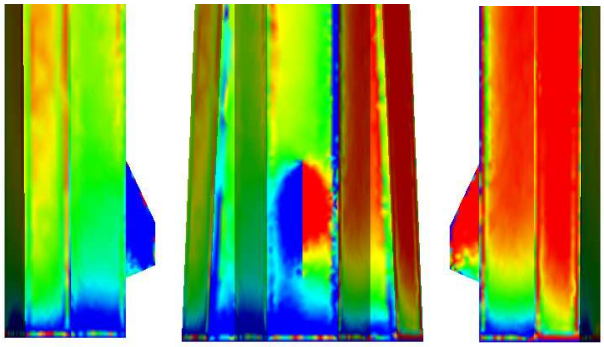

Figure 20. KROPP afterbody, fin at 50 cm. C_p. M = 0.5. α = 0 deg, β = -10 deg.

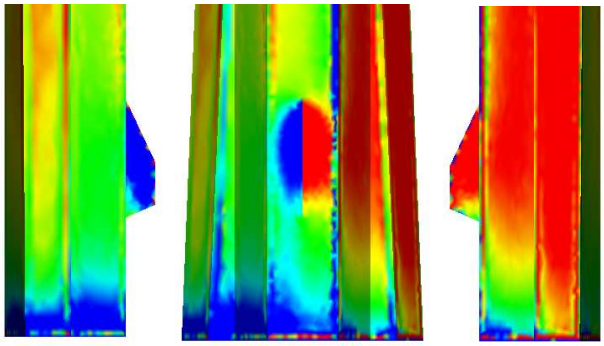

Figure 21. KROPP afterbody, fin at 75 cm. C_p. M = 0.5. α = 0 deg, β = -10 deg.

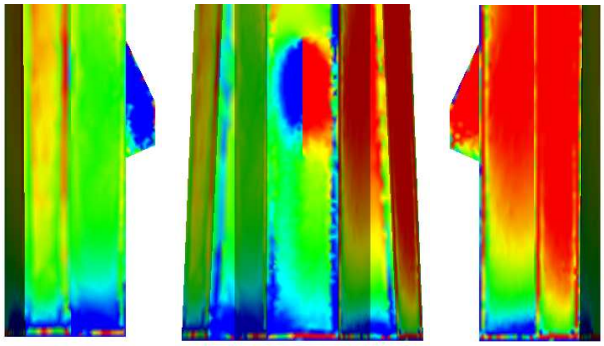

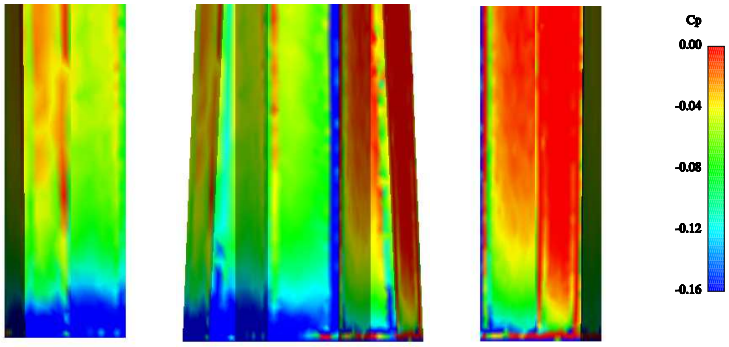

Figure 22. KROPP afterbody, no fin. M = 0.5. α = 0 deg, β = -10 deg.

CFD calculations As explained in chapter 3, the CFD results for Mach 0.5 were obtained with adapted grids. It was shown for the case with the fin at 50 cm that C_C and C_n are very close to zero for β = 0. Therefore, no calculations were made for β = 0 for the other cases, but the asymmetric forces and moments were assumed to be zero.

Results for all four fin positions show that even the very existence of a fin does not influence C_C much (figure 23). C_n shows the same pattern as for Mach 1.5: the body alone is unstable, addition of a fin makes it just stable (figure 24).

Looking at the fin Δ effects (figures 27 and 28), we see that some fin positions decrease the sideforce C_C, although windtunnel results show an increase in C_C. Windtunnel and CFD results show a comparable ΔC_n.

It can be seen that the fin effects are different for β = 0 – 5 deg and for β = 5 – 10 deg. This is most obvious from the approximated derivatives (figure 29 and 30, for a definition see section 4.2). The 5 – 10 lines show a maximum in $\Delta C_{C_{\beta,fin}}$ and $\Delta C_{n_{\beta,fin}}$ for the fin at 25 cm and the same values for 0 and 50 cm, while the 0 – 5 lines show a minimum at 25 cm and an increase towards 75 cm.

The accuracy of especially the derivative calculations is uncertain. Unlike the supersonic case, the flow around the fin is influenced by the base flow which is dependent on viscosity and therefore not predicted correctly by Euler calculations. And, because the effects of a little fin are so small, even minor errors have the same order of magnitude as the fin effects. The fact that CFD does not give an increase in C_C when a fin is added and the derivatives for β 0 – 5 and β 5 –10 that show different behaviour may be caused by numerical errors.

Best fin position Windtunnel results show a small dependence of C_C and C_n on fin position. CFD results indicate that the fin must be placed far forward for low β, but at about 25 cm for higher β. A maximum $\Delta C_{n_{\beta,fin}}$ of 0.39 is reached there, 16% higher than for the most backward position. Because of the uncertainty regarding the computational results, no specific conclusion of best fin position can be drawn. It is however reasonable to state that, for subsonic speeds, the effectiveness of the fin is rather independent of its position.

Windtunnel results for higher β show a slightly larger yawing moment when the fin is placed away from the base. The fin causes a pressure difference on the body behind it, which disappears when the fin is placed with its trailing edge at the body base. It is therefore recommended to place the fin at a small distance from the base.

Figure 23. Side force coefficient C_C versus β for α = 0, M = 0.5. Five different CFD calculations.

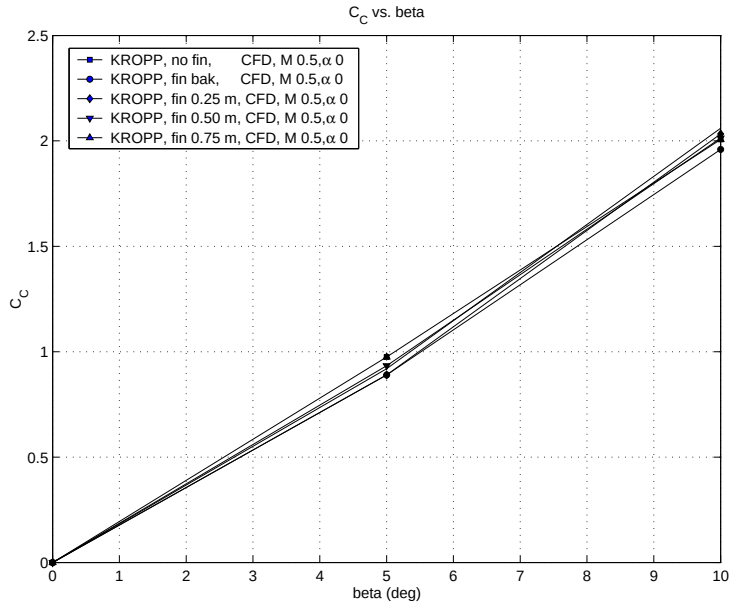

Figure 24. Yawing moment coefficient C_n versus β for α = 0, M = 0.5, five different CFD calculations.

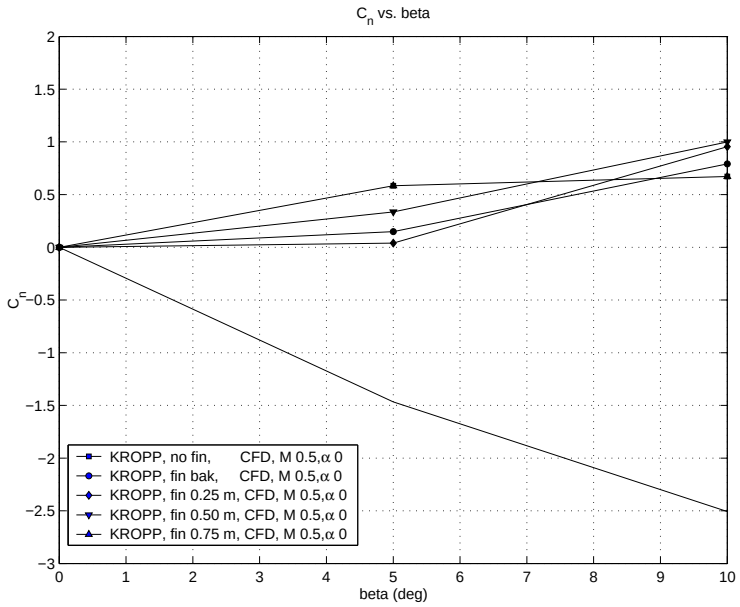

Figure 25. Side force coefficient C_C versus β for α = 0, M = 0.5. Comparison CFD – windtunnel.

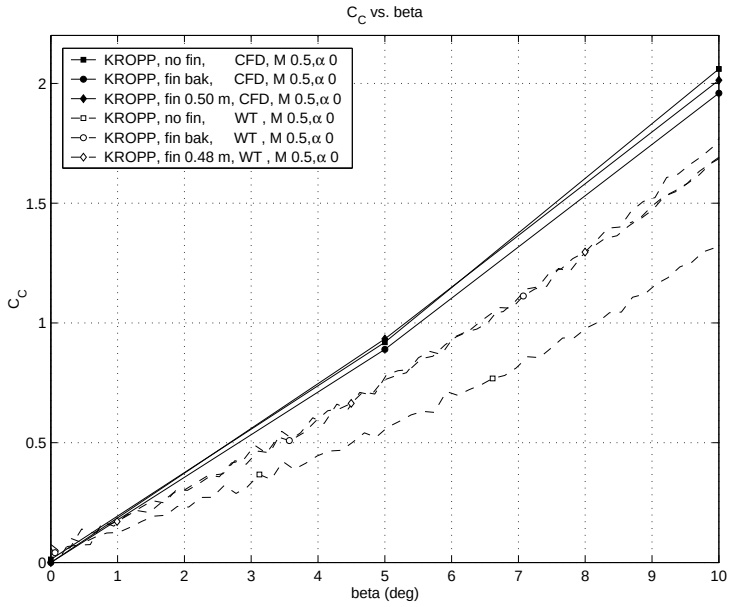

Figure 26. Yawing moment coefficient C_n versus β for α = 0, M = 0.5, comparison CFD – windtunnel.

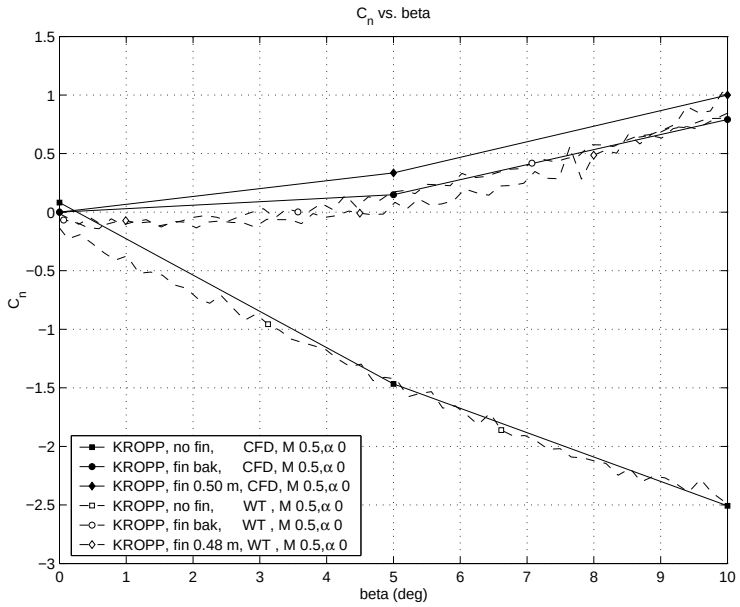

Figure 27. Side force coefficient with fin minus without fin, $\Delta C_{C,fin}$, versus β for α = 0, M = 0.5.

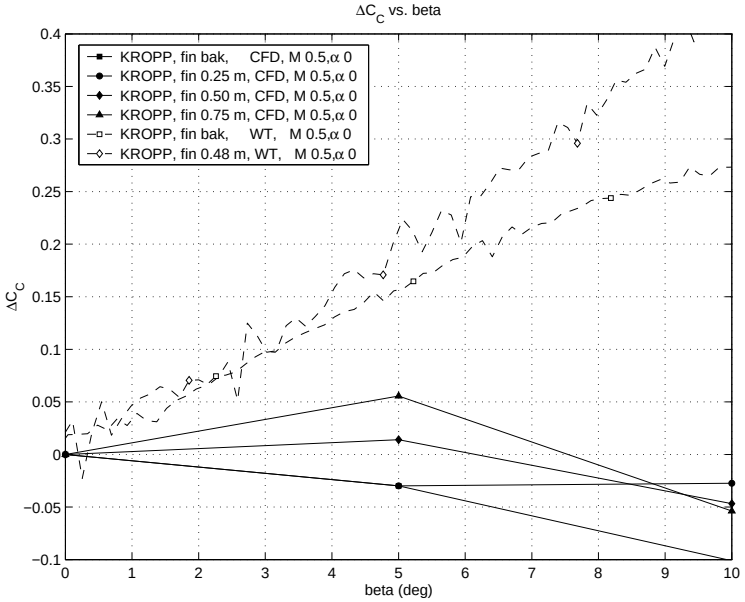

Figure 28. Yawing moment coefficient with fin minus without fin, $\Delta C_{n,fin}$, versus β for α = 0, M = 0.5.

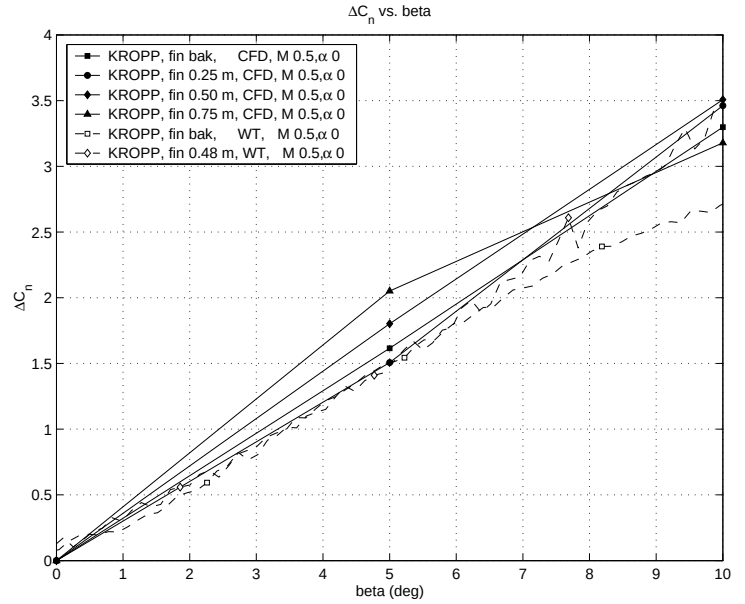

Figure 29. Side force derivative caused by fin, $\Delta C_{C_{\beta,fin}}$, versus distance base – fin trailing edge. M = 0.5

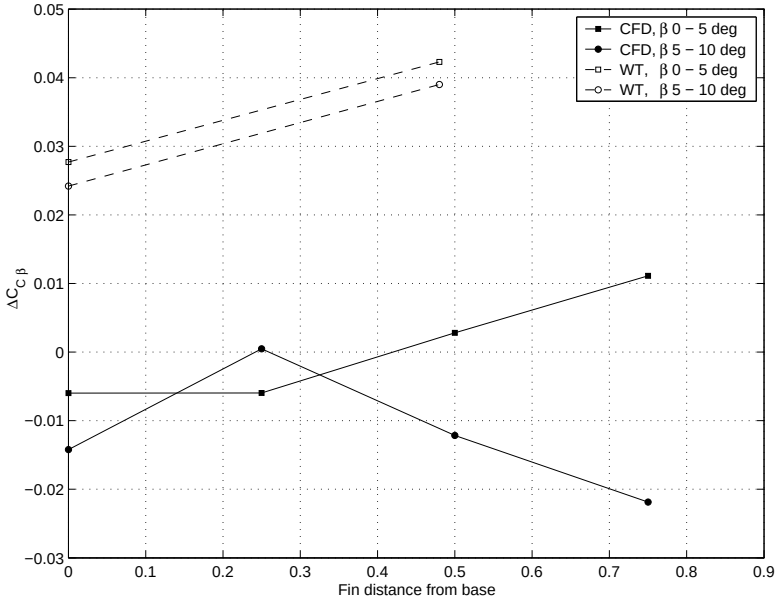

Figure 30. Yawing moment derivative caused by fin, $\Delta C_{n_{\beta,fin}}$, versus distance base – fin trailing edge. M = 0.5

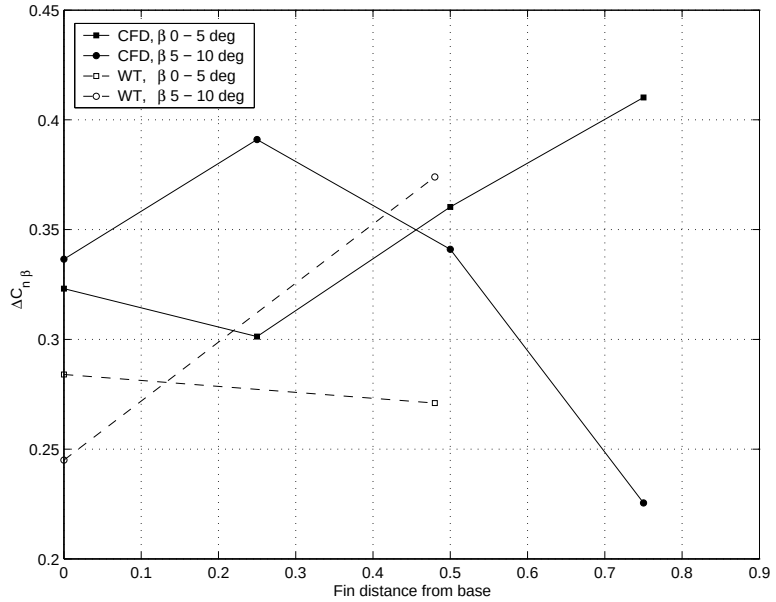

6 Conclusion

CFD calculations and windtunnel measurements were used to determine the optimum position of a small fin on a missile body to give maximum directional stability. To achieve sufficient accuracy, CFD calculations were performed on flow-adapted grids for subsonic speeds. This was not necessary for supersonic speeds.

At Mach 1.5 a wave pattern is formed on the body behind the fin. Maximum yawing moment is reached when this pattern is entirely free from the base area, this means that the fin must have its trailing edge between 50 and 75 cm from the base area. Calculations show an increase of yawing moment, caused by the fin, of 35%. It was found that, for higher angles of sideslip, the fin must be moved further forward.

For subsonic speeds, at Mach 0.5, the influence of the fin is limited to a small area around the fin. The horizontal underside of the missile is influenced most. The lower sides of the missile show a small pressure change close to the fin, they contribute thus to the yawing moment. It was found that the yawing moment does not change much with the fin position. Due to computational difficulties the correctness of the CFD-results is uncertain, but it is likely that there is an optimum position with the fin trailing edge a short distance away from the base.

References

[1] T. Sjögren and P. Eliasson, *Description and Validation of EDGE An edge-based Euler solver for unstructured grids*, FFA-TN 1998-61, FFA, Flygtekniska Försöksanstalten, 1998

[2] L.G. Tysell and S.G. Hedman, *Towards a General Three-dimensional Grid Generation system*, ICAS-88-4.7.4

[3] Lars G. Tysell, *An Advancing Front Grid Generation system for 3D Unstructured Grids*, ICAS-94-2.5.1

[4] Johannes Johansson, Dag Eriksson, Ola Hamnér and Rolf Jarlås, *Tvärteknikprojektet, Modellgeometrier för Vindtunnelprov 1*, FOI-D–0010–SE, FOI, Totalförsvarets Forskningsinstitut, 2001

Issuing organisation
FOI – Swedish Defence Research Agency
Division of Aeronautics, FFA
SE-172 90 STOCKHOLM

Report number, ISRN
FOI-R–0367–SE

Report type
Technical report

Month year
Jan 2002

Project number
E840264

Customers code
3. Aeronautical Research

Research area code
7. Vehicles

Sub area code
73. Aeronautical research

Author(s)
Jeroen Wackers

Project manager
Ola Hamnér

Approved by
Torsten Berglind
Head, Computational Department

Scientifically and technically responsible
Ola Hamnér
Computational Department

Report title
Position of a Small Fin on a Missile Body for Maximum Directional Stability

Abstract
Windtunnel measurements and CFD calculations were performed to determine the position of a small fin on a missile body that gives the highest directional stability. The model used is the configuration KROPP of the Tvärteknikprojekt, a concept for a future heavy cruise missile.
For supersonic speeds, the fin creates a shock pattern behind itself on the body. The generated pressure differences contribute to the yawing moment at sideslip, so much that it is advantageous to move the fin forward on the body. Although this decreases the effect of the fin itself (because of a shorter moment arm), it increases the total moment. The maximum yawing moment is encountered when the entire shock pattern is placed on the body. A 35% increase in yawing moment due to fin was noted.
For subsonic speeds this effect is smaller, because the fin influences a smaller part of the body. The yawing moment does not vary much with fin position. The best position is most probably with the trailing edge a short distance away from the base.

Keywords
fi n, missile, directional stability, yawing moment, body interference

Further bibliographic information

ISSN
ISSN 1650-1942

Pages
36

Language
English

Price
Acc. to price list

Security classification
Unclassifi ed

Utgivare	Rapportnummer, ISRN	Klassificering
Totalf¨orsvarets Forskningsinstitut – FOI Avdelningen f¨or Flygteknik, FFA SE-172 90 STOCKHOLM	FOI-R–0367–SE	Teknisk rapport
	Månad år Jan 2002	Projektnummer E840264
	Verksamhetsgren 3. Flygteknisk forskning	
	Forskningsområde 7. Bemannade och obemannade farkoster	
	Delområde 73. Flygteknisk forskning	
Författare Jeroen Wackers	Projektledare Ola Hamnér	
	Godkänd av Torsten Berglind Chef, Ber¨akningsaerodynamik	
	Tekniskt och/eller vetenskapligt ansvarig Ola Hamnér Ber¨akningsaerodynamik	

Rapporttitel

Placering av en liten fena på en robotkropp f¨or maximal girstabilitet

Sammanfattning

Vindtunnelmätningar och CFD-beräkningar har gjorts för att hitta den placering av en liten fena på en robotkropp som ger den största girstabiliteten. Konfiguration KROPP av Tvärteknikprojektet, en koncept för en framtida tung attackrobot, har studerats.

För överljudhastigheter bildar fenan en vågbild bakom sig på kroppen. Den ger tryckskillnader som ökar girmomentet, så mycket att det lönar sig att flytta fenan framåt på kroppen. Fastän fenans egen effekt minskar, blir det totala momentet större. Girmomentet blir maximalt när hela vågbilden kommit in på kroppen. Då blir fenans effekt 35% större.

För underljudhastigheter är effekten mindre, därför att fenan påverkar en mindre del av kroppen. Girmomentet ändrar sig inte mycket med fenans position. Fenans bästa position är antagligen med bakkanten en liten distans från basytan.

Nyckelord

fena, robot, girstabilitet, girmoment, kroppsinterferens

Övriga bibliografiska uppgifter

ISSN	Antal sidor	Språk
ISSN 1650-1942	35	Engelska
Distribution enligt missiv	Pris Enligt prislista	
	Sekretess Öppen	